FE^2 modelling of solids undergoing strain localization

Wenjin Xing[1,a *], Anthony Dennis Miller[1,b], Stuart Wildy[1,c], John Codrington[2,d]

[1]School of Computer Science, Engineering and Mathematics, Flinders University, Australia

[2]School of Mechanical Engineering, University of Adelaide, Australia

[a]xing0029@flinders.edu.au, [b]tony.miller@flinders.edu.au

[c]stuart.wildy@flinders.edu.au, [d]john.codrington@adelaide.edu.au

Keywords: Multiscale modelling; computational homogenization; strain localization; scale transitions; boundary conditions.

Abstract. This present contribution is concerned with exploring a computational homogenization scheme and an appropriate BC for accurately modelling two-scale failure problems. Variationally Consistent Homogenization (VCH) paradigm as the backbone theory is adopted. Different prolongation strategies are postulated to treat intact and fractured subregions at the macroscale. The weak formulation for the fracture macroscale problem is derived, wherein the constitutive laws are homogenized from the microscale computation. The tessellation BC, enforced on the microscale problem, is used to obtain an accurate localization zone development at the microscale and an effective stiffness prediction. The examples given indicate that the proposed FE^2 scheme is able to handle arbitrary localization directions and produces solutions that are insensitive to the statistical volume element (SVE) size and the macroscopic mesh.

1 Introduction

Structural and material failure is generally a multiscale phenomenon. Macroscopically observed failure is often accompanied by damage events or material instabilities occurring at smaller scales. This is usually a strong coupling process, which fits in well with a concurrent multiscale modelling framework [1].

However, when resolving such failure by computational homogenization schemes (termed FE^2, when finite elements are used at both scales), it is well recognized that the classical FE^2 approach fails. This is because the scale separation rule no longer holds and the representative volume element (RVE) loses its representative character for regions experiencing strong strain localizations which arise from material softening in narrow regions of the solid. In the literature, several novel ideas or numerical formulations have been proposed to extend the classical homogenization scheme to overcome such challenges in the framework of FE^2. Representative works include Belytschko et al. [2], Verhoosel et al. [3], Nguyen et al. [4], Coenen et al. [5], Bosco et al. [6], Toro et al. [7], Svenning et al. [8], Souza et al. [9], to name a few. Most of these works attempt to extract from the microscale problem an objective effective macro crack response, which is governed by traction-separation laws.

The finite element (FE) solution for solving material softening problems suffers from pathological mesh size dependence, due to the fact that the stress governing equations lose ellipticity upon the onset of the strain localization. To circumvent the macroscale mesh sensitivity, a kinematics enhanced continuum description is necessary. Thereby, different existing discrete crack modelling approaches can be used to allow for the insertion of a discontinuity. The extended finite element method (X-FEM) was adopted in [2, 4, 6, 8]. However, element embedded discontinuities approach was used in [5, 7] and cohesive elements by Verhoosel et al. [3].

Boundary conditions (BCs) for the SVE (in this article, we term the micro cell as statistical volume element instead of representative volume element) are another concern in the macro-to-micro transition in computational homogenization schemes. Improper designs or choices will significantly affect the homogenized effective quantities and responses at both scales. This becomes more stringent upon strain localization. Commonly used kinematic BCs in the classical computational homogenization include linear displacement, periodic, and minimal kinematic BC. If strain

localization occurs in the SVE, all these provide an unrealistic localization pattern in terms of its opening across the SVE boundary and inexact effective material response [10]. To this end, many investigations have been undertaken [11, 12, 13, 14, 17]. The periodicity frame is adjusted to accommodate the localization development in the SVE. This is done adaptively in [12, 14] by the detection of potential dominant localization bands using Hough transform before and after the loss of stability. Moreover, to overcome the inconvenience induced by non-congruent SVE meshes after a change of the frame, a noticeable similar idea for a majority of these works is to apply the shifted periodic correspondence in a weak/integral sense instead of pointwise. Goldmann et al. in [14] compared five different BCs for SVE undergoing localization, including his proposed tessellation BC. Besides permitting arbitrary development of localization zones, the tessellation BC is also unsusceptible against spurious localization.

The remainder of this article is organized as follows. In section 2, the single scale problem is described and its weak form is given. The section 3 presents the multiscale formulation based on the VCH, the applied tessellation BC and the possible algorithms for the detection of a strong localization band on the softening SVE. Two benchmark examples are provided with direct numerical simulations (DNS) as a reference solution in the section 4, followed by the conclusion section 5.

2 Problem description

Let us consider a homogeneous body occupying Ω in two dimensional Euclidean space. The material particle at each point in the body is denoted by $\boldsymbol{X}$ and its position by $\boldsymbol{x}$ in the deformed configuration. A cohesive crack is embedded in the body, which is a two-sided interface Γ_{int}, shown in Fig. 1. The crack and its virtual extension separates the domain into two parts, negative and positive parts, signed with -/+. A Dirichlet type BC $\overline{\boldsymbol{u}}$ is prescribed on the external displacement boundary $\partial\Omega u$; a Neumann type BC $\overline{\boldsymbol{t}}$ is enforced on the external traction boundary $\partial\Omega t$, with outward normal $\mathbf{n}$. Also, $\partial\Omega u \cup \partial\Omega t = \partial\Omega$, $\partial\Omega u \cap \partial\Omega t = \phi$. The cohesive crack experiences tractions on its two faces, which depend on the displacement jump (crack opening) across the crack. Here, we just refer to the quasi-static case and there is no body force. Small strain condition is assumed.

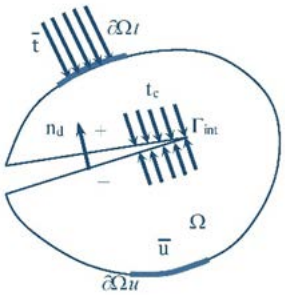

Fig. 1 A 2D solid with a cohesive crack.

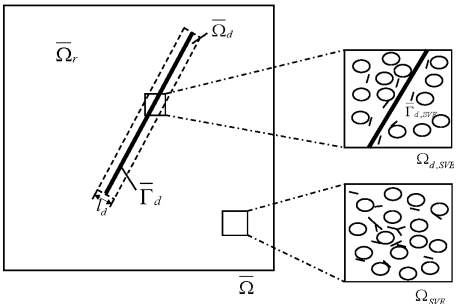

Fig. 2 Dividing the macroscopic domain into two parts, $\overline{\Omega}_r$ and $\overline{\Omega}_{\text{d}}$ (left). Each has a characteristic microstructure. A SVE is experiencing material softening (right top) and a SVE is in a state prior to loss of stability (right below).

The single (displacement) field weak formulation for such a fracture problem is derived as

$$\text{find } \boldsymbol{u} \in \text{U } s.t. \;\; a(\boldsymbol{u}, \delta\boldsymbol{u}) - b(\boldsymbol{t}\{[\![\boldsymbol{u}]\!]\}, \delta\boldsymbol{u}) = l(\delta\boldsymbol{u}) \qquad \forall\ \delta\boldsymbol{u} \in \text{U}^0, \tag{1}$$

$$a(\boldsymbol{u}, \delta\boldsymbol{u}) = \int_{\Omega} \boldsymbol{\sigma} : [\delta\boldsymbol{u} \otimes \nabla]^s \, d\Omega \,,$$

$$b(\boldsymbol{t}\{[\![\boldsymbol{u}]\!]\}, \delta\boldsymbol{u}) = \int_{\Gamma_{\text{int}}} \boldsymbol{t}\{[\![\boldsymbol{u}]\!]\} \cdot [\![\delta\boldsymbol{u}]\!] \, d\Gamma \,, \tag{2)(3)(4}$$

$$l(\delta\boldsymbol{u}) = \int_{\partial\Omega t} \bar{\boldsymbol{t}} \cdot \delta\boldsymbol{u} \, d\Gamma,$$

where $[\![\boldsymbol{u}]\!]$ and $\boldsymbol{t}\{[\![\boldsymbol{u}]\!]\}$ denote the displacement jump and cohesive traction on the crack surfaces, respectively and where U is a trail function space from which we seek the FE approximate solution and U^0 is the corresponding admissible test function space.
The above physical problem can be solved directly with FE once the bulk material and cohesive crack constitutive laws are known. However, in practice, the theoretical derivation of such constitutive laws becomes intractable for highly heterogeneous and hierarchical materials. Furthermore, the solution obtained through a full resolution of microstructure details with a fine enough mesh is very computational demanding. To avoid these difficulties, we pursue a smooth solution to this weak formulation through a computational multiscale scheme.

3 Multiscale formulation

3.1 Variationally consistent homogenization (VCH)

The VCH approach resembles Variational Multiscale Methods (VMM) by Hughes et al. [16]. The first step of VCH is to additively split the solution in U into macro (M) and micro (s) counterparts. The same split applies to any test functions in U^0. Making splits, we are able to reinterpret the original problem as the macro Eq. (5) and the micro problem Eq. (6) as follows

$$\begin{aligned} &a(\boldsymbol{u},\delta\boldsymbol{u}^M)-b(\boldsymbol{t}\{[\![\boldsymbol{u}]\!]\},\delta\boldsymbol{u}^M)=l(\delta\boldsymbol{u}^M)\ \ \forall\delta\boldsymbol{u}^M\in\mathrm{U}^{M,0}\,,\\ &a(\boldsymbol{u},\delta\boldsymbol{u}^s)-b(\boldsymbol{t}\{[\![\boldsymbol{u}]\!]\},\delta\boldsymbol{u}^s)=l(\delta\boldsymbol{u}^s)\ \ \forall\delta\boldsymbol{u}^s\in\mathrm{U}^{s,0}\,, \end{aligned} \qquad (5)\ (6)$$

where we recall that bilinear forms $a(\bullet,\bullet)$, $b(\bullet,\bullet)$ and linear functional $l(\bullet)$ were defined in Eqs. (2), (3) and (4), respectively. Then we need to localize the above equations onto each SVE. This is achieved by using running averages [8, 17] .We use $\overline{\Omega}_r$ and $\overline{\Omega}_d$ to represent the macroscopic region with the material prior to strain localization (loss of stability) and undergoing strain localization, respectively, shown in Fig. 2. Note that there are two different types of SVEs in terms of computational homogenization, one for $\overline{\Omega}_r$ and the other for $\overline{\Omega}_d$.

Next, prolongation conditions are defined to bridge the macroscale part of the SVE deformation and the homogenized (smooth) solution we are looking for. For ease of description, notation $\overline{(\bullet)}$ indicates quantities that pertain to the macroscopic domain where the homogenization/averaging procedure has been exploited. For SVEs within $\overline{\Omega}_r$, the conventional first order homogenization is employed,

$$\boldsymbol{u}^M=\overline{\boldsymbol{u}}+\boldsymbol{\varepsilon}\left[\overline{\boldsymbol{u}}(\overline{\boldsymbol{x}})\right]\cdot(\boldsymbol{x}-\overline{\boldsymbol{x}})\quad\forall\overline{\boldsymbol{x}}\in\overline{\Omega_r}\,, \qquad (7)$$

where $\overline{\Omega_r}$ denotes the homogenized domain and $\overline{\boldsymbol{u}}(\overline{\boldsymbol{x}})$ is the smooth solution at the $\overline{\boldsymbol{x}}$.

For SVEs located in $\overline{\Omega}_d$, as mentioned before, the classical averaging theorems do not hold any longer. The displacement field across the macroscale strong discontinuity is discontinuous and the resulting infinite strain does not make sense when using the assumption Eq. (7). Considering the equivalence between a strong discontinuity and a smeared weak discontinuity under the nonlinear fracture mechanics, we may smear the strong discontinuity jump over a certain dimension that is the SVE width under localization. In other words, we lump the microscale strain localization band from the strain localized SVE into a macroscale cohesive crack. This operation coincides with that Svenning et al. [8] populated the entire domain $\overline{\Omega}_d$ with SVEs through the width l_d . After taking the smeared approach, the macroscale part of the SVE displacements has the form [5, 8]

$$\boldsymbol{u}^M = \bar{\boldsymbol{u}} + \bar{\boldsymbol{\varepsilon}}_d \cdot (\boldsymbol{x} - \bar{\boldsymbol{x}}) \quad \forall \bar{\boldsymbol{x}} \in \overline{\Gamma_d},$$
$$\bar{\boldsymbol{\varepsilon}}_d = \bar{\boldsymbol{\varepsilon}}_0 + \frac{1}{2l_d}\left(\left[\!\left[\bar{\boldsymbol{u}}\right]\!\right] \otimes \boldsymbol{n} + \boldsymbol{n} \otimes \left[\!\left[\bar{\boldsymbol{u}}\right]\!\right]\right), \tag{8) (9) (10)}$$
$$l_d = \frac{\left|\Omega_{d,SVE}\right|}{\left|\overline{\Gamma}_{d,SVE}\right|},$$

where $\bar{\boldsymbol{\varepsilon}}_0$ denotes the effective bulk strain of the material surrounding the macroscale crack, $\bar{\boldsymbol{\varepsilon}}_d$ indicates the average strain that represents the sum of the strain contributions due to the bulk and the macroscale discontinuity jump within $\overline{\Omega}_d$, respectively and l_d is the smearing width.

The fluctuation term that arises from the existence of the displacement discontinuity in the macroscopic domain is taken into account at the microscale due to such a definition of the average strain. Moreover, Eq. (9) relates the average strain for the localized SVE to the SVE size such that an objective effective response independent of arbitrary SVE sizes is ensured.

Note that in Fig. 2, $\overline{\Omega}_r$ and $\overline{\Omega}_d$ should not overlay each other, which leads to inconvenience in the computational implementation. As discussed in [8], we transform the integral over $\overline{\Omega}_r$ into an approximate integral over the whole macroscopic (continuous) domain $\widehat{\Omega}$ excluding the discontinuous cohesive crack.

After approximating integrals in the weak formulation, specifying prolongation conditions, and making an approximate transformation of the integral over $\overline{\Omega}_r$, Eq. (6) is rephrased as [8]

$$\int_{\hat{\Omega}} \bar{\boldsymbol{\sigma}}\left\{\boldsymbol{\varepsilon}\left[\bar{\boldsymbol{u}}\right]\right\} : \boldsymbol{\varepsilon}\left[\delta\bar{\boldsymbol{u}}\right] d\Omega + \int_{\overline{\Gamma}_d} l_d \bar{\boldsymbol{\sigma}}\left\{\bar{\boldsymbol{\varepsilon}}_d\right\} : \left(\left[\!\left[\delta\bar{\boldsymbol{u}}\right]\!\right] \otimes \boldsymbol{n}\right)^s d\Gamma = l(\delta\bar{\boldsymbol{u}}) \;\; \forall\, \delta\bar{\boldsymbol{u}} \in \bar{U}^0,$$
$$\bar{\boldsymbol{\sigma}}\{\bullet\} = \frac{1}{\left|\Omega_{r/d,SVE}\right|} \int_{\Omega_{r/d,SVE}} \boldsymbol{\sigma} \, d\Omega. \tag{11) (12)}$$

Note that we have ignored a correction term (cf. [8]) by assuming l_d is small enough compared to the macroscale characteristic dimension and the deformation neighbouring the macroscale crack is nearly homogeneous. This is the case for quasi-brittle materials because typically elastic unloading happens in the bulk material in $\overline{\Omega}_d$. Eq. (11) corresponds to the second alternative formulation in [8]. The second term represents the cohesive contribution for the macroscale crack whose constitutive law originates from the homogenization over a strain localized SVE. Obviously, compared to the first alternative in [8], this formulation appears unsymmetric but does not require duplicated SVEs in the Gauss points on $\overline{\Gamma_d}$. To implement Eq. (11) the with FE method, linearization of the (homogenized) stresses is done through condensation processes to get effective tangent stiffnesses required in Newton's iterative solver.

3.2 Tessellation BCs on localized SVE

As argued in the introduction section, precise BCs are a necessity to produce fast converged effective quantities as the increasing SVE size. Prior to the occurrence of material instability, the BC will affect the direction and the position of the emerging localization band. Furthermore, upon localization, the strain localization profile across the SVE boundary is also dominated by the BC. To achieve an accurate localized SVE response, the tessellation BC [14] is employed. The primary idea behind this tessellation BC is to redefine the periodicity frame that aligns with the normal of the localization band.

Due to inconsistency between the opposite boundary meshes, instead of a nodewise correspondence, the integral (weak) form is applied at the microscale

$$\int_{\partial\Omega^{+}_{m,j}} \boldsymbol{u}\, d\Gamma - \int_{\partial\Omega^{-}_{m,j}} \boldsymbol{u}\, d\Gamma = \bar{\boldsymbol{\varepsilon}} \cdot \left(\int_{\partial\Omega^{+}_{m,j}} \boldsymbol{x}\, d\Gamma - \int_{\partial\Omega^{-}_{m,j}} \boldsymbol{x}\, d\Gamma\right), \tag{13}$$

where m = 1,2 indicate the direction along which the division is performed and sign +/- denote the two opposite boundaries. The subscript j represent the integration zones on which the above integral equality has to hold separately. For m = 2, the case is depicted in Fig. 3.

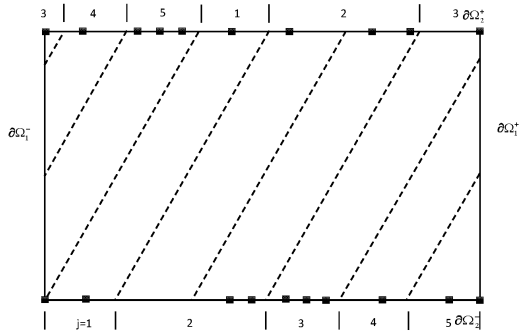

Fig. 3 Tesselation BC for an oblique angle. Black squares symbolize nodes. Dashed lines show a preliminary division of the upper and the lower boundary into integration zones along m = 2. Zones 1~5 are the final division to ensure every integration zone poessesses at least one node per side.

Typically, penalty method or Lagrange multiplier method can be used to implement the above integral Eq. (13). However, with the penalty method, care must be taken to adopt a proper value for penalty parameters since too large a value may cause the global stiffness matrix bad-conditioned and too small a value gives poor accuracy on solution. To this purpose, the Lagrange multiplier method is used. This leads to a mixed formulation for the SVE boundary value problem, for which the inf-sup stability condition has to be fulfilled to justify stability.

If constant traction elements were used to discretise the Lagrange multiplier field, as argued in [17], each constant traction element must correspond to at least two linear displacement elements, which demands that in each integration zone at least one displacement node exists. That is the reason why we should check for a preliminary division.

3.3 Strong Localization detection algorithm

There exist multiple strategies to distinguish the dominant strain localization. Herein, two alternatives are taken into account.

3.3.1 Strong ellipticity condition

When a discontinuity interface appears at material points, the tangent stiffness tensor will lose the nature of strong ellipticity [2]. As a result, the criterion is written as

$$\det(\mathbf{n}\cdot\mathbf{C}^{4}_{M}\cdot\mathbf{n}) = \det(\mathbf{Q}) \le 0\,, \tag{14}$$

wherein the $\mathbf{Q} = \mathbf{n}\cdot\mathbf{C}^{4}_{M}\cdot\mathbf{n}$ is a second order tensor referred to as acoustic tensor. This can be used to detect the instance when a macroscale crack segment occurs and the normal direction to this emerging crack segment.

3.3.2 Hough transform

Due to the fact that the accurate strain localization development prior to loss of the strong ellipticity is also crucial, the adjustment of the periodicity frame adaptively to reduce the spurious interference with the strain localization development and profile on the SVE of the boundary condition is necessary, which may require a constant detection process of the dominant strain localization direction. This can be accomplished by means of the Hough transform technique. However, in this contribution, we only pay attention to the post-critical phase, meaning that it may be utilized after post localization as an alternative. The underlying idea of using Hough transform in the FE^2 setting for failure is the equivalent strain field can be regarded as an image, from which it is possible to extract the approximately straight band which covers the highest equivalent strain distribution. Interested readers can refer to literature [12, 14] for more details.

4 Numerical examples

4.1 Specimen with a vertical softening (voided) band

This benchmark test is designated to show the validity of the proposed FE^2 scheme. The geometry of the specimen is illustrated in Fig. 4 and the meshes for DNS and FE^2 simulation are shown in Fig. 5.

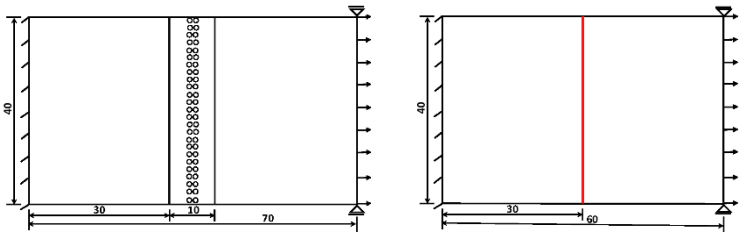

Fig. 4 Geometry of the specimen for the benchmark problem 4.1 (all units in mm): DNS (left) and macroscale in FE^2 (right). The accumulation of voids represents the softening and the red line indicates a cohesive crack.

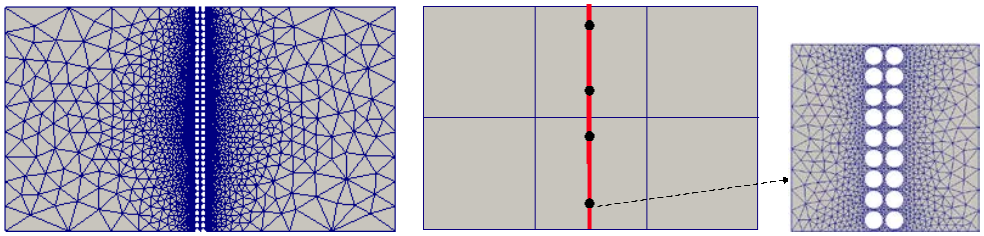

Fig. 5 The discretizations for the DNS (left), the macroscale problem (middle) and the SVE (right) attached to a cohesive zone integration point marked with black dot.

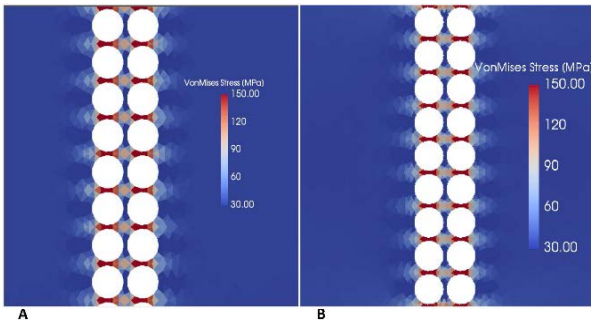

Fig. 6 Von Mises effective stress distribution: (A) on a portion of the voided band in the DNS and (B) on a SVE in the FE^2 simulation

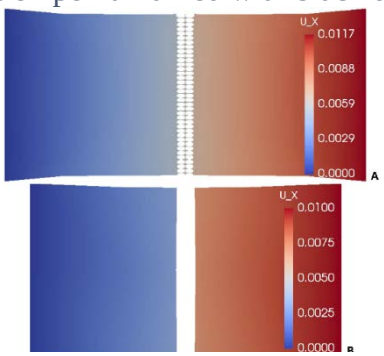

Fig. 7 Horizontal displacements on the deformed configuration (X 1000): (A) for the DNS and (B) for the macroscale problem (FE^2).

A comparison of the Von Mises effective stress field between the DNS and the FE^2 simulation is given in Fig. 6. Also, horizontal displacements on the magnified deformed configurations are presented in Fig. 7 to support the effectiveness of the FE^2 scheme.

4.2 Elastic plate with an inclined effective localization band

To further investigate the SVE size dependence for the current discontinuity kinematics enhanced multiscale scheme and the utility of the implemented tessellation BC, an elastic plate with an inclined strain localization band is considered, shown in Fig. 8. Also given are the boundary conditions with u_x equal to ***0.01 mm*** . The localization band is modelled by a softener material with a modulus ratio of ***0.1*** to that of the bulk material. Plane strain is assumed. For the FE^2 simulation, the macroscale discontinuity is modelled with XFEM. The discontinuity in the microscale problem is characterized

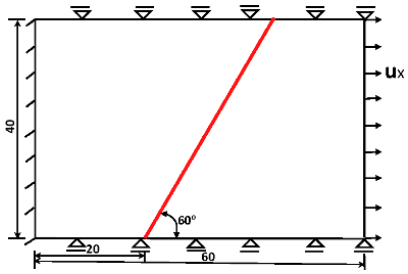

Fig. 8 Geometry of the elastic plate with a cohesive crack (4.2).

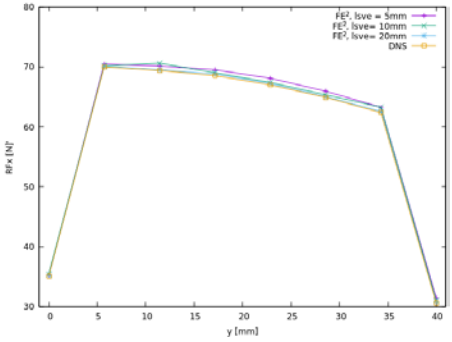

Fig. 9 Horizontal reaction forces along the right edge under tension.

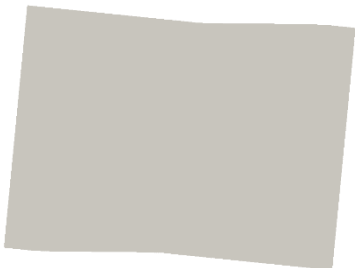

Fig. 10 Deformed SVE (10 x 10 mm^2) under strain localization, magnified by a factor of 400.

by the inclined effective localization band.

Horizontal reaction forces on the right edge obtained from FE^2 simulations with three different SVE sizes (side length = 5, 10, 20) are compared with the DNS solution to illustrate the size independence of the FE^2 scheme as shown in Fig. 9. The Hough transform technique (see 3.2.2) is applied for the FE^2 to detect the strain localization orientation in order to enforce the tessellation BC that is aligned with the orientation of the localization band. A deformed SVE undergoing strain localization is shown in Fig. 10, from which we are able to justify the "tessellation" character.

5 Conclusions

This work presented employed the VCH paradigm, a smeared macro to micro discontinuity transition and a tesselation BC to allow for strain localization with arbitrary directions in solids. Two preliminary simple examples with an assumed softening band on the SVE were studied to demonstrate its validity. However, continuum damage models and cohesive elements can be considered for defining a more realistic microscale problem. Like any FE^2 methods, the computational cost for the application of this FE^2 scheme is still very budernsome compared to simulations with postulated macroscopic constitutive laws. Parallel computing and model reduction strategies are potential approaches to enhance the speed of the FE^2 simulations with applications to real life engineering problems, such as concrete failure analysis, cortical bone fracture mechanism investigation, invention of novel heterogeneous materials.

References

[1] Hettich, T., Hund, A. and Ramm, E., 2008. Modeling of failure in composites by X-FEM and level sets within a multiscale framework. *Computer Methods in Applied Mechanics and Engineering*, *197*(5), pp.414-424.

[2] Belytschko, T., Loehnert, S., & Song, J. H. (2008). Multiscale aggregating discontinuities: a method for circumventing loss of material stability. International Journal for Numerical Methods in Engineering, 73(6), 869-894.

[3] Verhoosel, C. V., Remmers, J. J., Gutiérrez, M. A., & De Borst, R. (2010). Computational homogenization for adhesive and cohesive failure in quasi-brittle solids. International Journal for Numerical Methods in Engineering, 83(8-9), 1155-1179.

[4] Nguyen, V. P., Lloberas-Valls, O., Stroeven, M., & Sluys, L. J. (2011). Homogenization-based multiscale crack modelling: from micro-diffusive damage to macro-cracks. Computer Methods in Applied Mechanics and Engineering, 200(9), 1220-1236.

[5] Coenen, E. W. C., Kouznetsova, V. G., & Geers, M. G. D. (2012). Multi-scale continuous–discontinuous framework for computational-homogenization–localization. Journal of the Mechanics and Physics of Solids, 60(8), 1486-1507.

[6] Bosco, E., Kouznetsova, V. G., & Geers, M. G. D. (2015). Multi-scale computational homogenization–localization for propagating discontinuities using X-FEM. International Journal for Numerical Methods in Engineering, 102(3-4), 496-527.

[7] Toro, S., Sánchez, P. J., Blanco, P. J., de Souza Neto, E. A., Huespe, A. E., & Feijóo, R. A. (2016). Multiscale formulation for material failure accounting for cohesive cracks at the macro and micro scales. International Journal of Plasticity, 76, 75-110.

[8] Svenning, E., Larsson, F., & Fagerström, M. (2017). Two-scale modeling of fracturing solids using a smeared macro-to-micro discontinuity transition. Computational Mechanics, 1-15.

[9] Souza, F. V., & Allen, D. H. (2011). Modeling the transition of microcracks into macrocracks in heterogeneous viscoelastic media using a two-way coupled multiscale model. International Journal of Solids and Structures, 48(22), 3160-3175.

[10] Inglis, H. M., Geubelle, P. H., & Matouš, K. (2008). Boundary condition effects on multiscale analysis of damage localization. Philosophical Magazine, 88(16), 2373-2397.

[11] Larsson, F., Runesson, K., Saroukhani, S., & Vafadari, R. (2011). Computational homogenization based on a weak format of micro-periodicity for RVE-problems. Computer Methods in Applied Mechanics and Engineering, 200(1), 11-26.

[12] Coenen, E. W. C., Kouznetsova, V. G., & Geers, M. G. D. (2012). Novel boundary conditions for strain localization analyses in microstructural volume elements. International Journal for Numerical Methods in Engineering, 90(1), 1-21.

[13] Svenning, E., Fagerström, M., & Larsson, F. (2017). Localization aligned weakly periodic boundary conditions. International Journal for Numerical Methods in Engineering.

[14] Goldmann, J., Brummund, J. and Ulbricht, V., On boundary conditions for homogenization of volume elements undergoing localization. International Journal for Numerical Methods in Engineering.

[15] Larsson, F. and Runesson, K., 2008. Adaptive bridging of scales in continuum modeling based on error control. International Journal for Multiscale Computational Engineering, 6(4).

[16] Hughes, T. J., Feijóo, G. R., Mazzei, L., & Quincy, J. B. (1998). The variational multiscale method—a paradigm for computational mechanics. Computer methods in applied mechanics and engineering, 166(1-2), 3-24.

[17] Svenning, E., Fagerström, M., & Larsson, F. (2016). Computational homogenization of microfractured continua using weakly periodic boundary conditions. Computer Methods in Applied Mechanics and Engineering, 299, 1-21.